J|A|C|S
ARTICLES

Published on Web 12/01/2010

Ferric Superoxide and Ferric Hydroxide Are Used in the Catalytic Mechanism of Hydroxyethylphosphonate Dioxygenase: A Density Functional Theory Investigation

Hajime Hirao[†,§] and Keiji Morokuma*[,†,‡]

Fukui Institute for Fundamental Chemistry, Kyoto University, 34-4 Takano Nishihiraki-cho, Sakyo, Kyoto 606-8103, Japan, and Cherry L. Emerson Center for Scientific Computation and Department of Chemistry, Emory University, Atlanta, Georgia 30322, United States

Received September 17, 2010; E-mail: morokuma@fukui.kyoto-u.ac.jp

Abstract: Hydroxyethylphosphonate dioxygenase (HEPD) is a mononuclear nonheme iron enzyme that utilizes an O_2 molecule to cleave a C−C bond in 2-hydroxyethylphosphonate and produce hydroxymethylphosphonate (HMP) and formic acid. Density functional theory calculations were performed on an enzyme active-site model of HEPD to understand its catalytic mechanism. The reaction starts with H-abstraction from the C2 position of 2-HEP by a ferric superoxide-type (Fe(III)-$OO^{\bullet-}$) intermediate, in a similar manner to the H-abstraction in the reaction of the dinuclear iron enzyme *myo*-inositol oxygenase. The resultant Fe(II)-OOH intermediate may follow either a hydroperoxylation or hydroxylation pathway, the former process being energetically more favorable. In the hydroperoxylation pathway, a ferrous-alkylhydroperoxo intermediate is formed, and then its O−O bond is homolytically cleaved to yield a complex of ferric hydroxide with a gem-diol radical. Subsequent C−C bond cleavage within the gem-diol leads to formation of an R-$CH_2^{\bullet}$ species and one of the two products (i.e., formic acid). The R-$CH_2^{\bullet}$ then intramolecularly forms a C−O bond with the ferric hydroxide to provide the other product, HMP. The overall reaction pathway does not require the use of a high-valent ferryl intermediate but does require ferric superoxide and ferric hydroxide intermediates.

1. Introduction

There is growing interest in a particular type of iron enzymes that utilize a ferric superoxide (Fe(III)-$OO^{\bullet-}$) intermediate to activate their substrates.[1,2] One of the best known examples of these enzymes is the nonheme diiron enzyme *myo*-inositol oxygenase (MIOX).[3] Spectroscopic analyses of MIOX have revealed that a (superoxo)Fe(III)Fe(III) intermediate acts as a reactive species when abstracting a hydrogen atom from the substrate.[4] X-ray crystal structures of MIOX showed that the abstracted hydrogen is positioned appropriately in the vicinity of the putative superoxo moiety.[5] The (superoxo)Fe(III)Fe(III)-type intermediate of MIOX has been theoretically characterized by the authors, and it has been demonstrated that the intermediate has H-abstraction ability.[6] Other examples of these enzymes include isopenicillin N synthase (IPNS)[7,8] and (*S*)-2-hydroxypropylphosphonic acid epoxidase (HppE).[9,10] These enzymes are different from taurine:α-ketoglutarate dioxygenase (TauD)[11] and cytochromes P450 (P450s),[12,13] which activate their sub-

† Kyoto University.
‡ Emory University.
§ Present address: Graduate School of System Informatics, Kobe University.

(1) Bollinger, J. M., Jr.; Krebs, C. *Curr. Opin. Chem. Biol.* **2007**, *11*, 151–158.
(2) Mukherjee, A.; Cranswick, M. A.; Chakrabarti, M.; Paine, T. K.; Fujisawa, K.; Münck, E.; Que, L., Jr. *Inorg. Chem.* **2010**, *49*, 3618–3628.
(3) Bollinger, J. M., Jr.; Diao, Y.; Matthews, M. L.; Xing, G.; Krebs, C. *Dalton Trans.* **2009**, 905–914.
(4) (a) Xing, G.; Hoffart, L. M.; Diao, Y.; Prabhu, K. S.; Arner, R. J.; Reddy, C. C.; Krebs, C.; Bollinger, J. M., Jr. *Biochemistry* **2006**, *45*, 5393–5401. (b) Xing, G.; Barr, E. W.; Diao, Y.; Hoffart, L. M.; Prabhu, K. S.; Arner, R. J.; Reddy, C. C.; Krebs, C.; Bollinger, J. M., Jr. *Biochemistry* **2006**, *45*, 5402–5412. (c) Xing, G.; Diao, Y.; Hoffart, L. M.; Barr, E. W.; Prabhu, K. S.; Arner, R. J.; Reddy, C. C.; Krebs, C.; Bollinger, J. M., Jr. *Proc. Natl. Acad. Sci. U.S.A.* **2006**, *103*, 6130–6135.
(5) (a) Brown, P. M.; Caradoc-Davies, T. T.; Dickson, J. M. J.; Cooper, G. J. S.; Loomes, K. M.; Baker, E. N. *Proc. Natl. Acad. Sci. U.S.A.* **2006**, *103*, 15032–15037. (b) Thorsell, A.-G.; Persson, C.; Voevodskaya, N.; Busam, R. D.; Hammarström, M.; Gräslund, S.; Gräslund, A.; Hallberg, B. M. *J. Biol. Chem.* **2008**, *283*, 15209–15216.
(6) Hirao, H.; Morokuma, K. *J. Am. Chem. Soc.* **2009**, *131*, 17206–17214.
(7) Brown, C. D.; Neidig, M. L.; Neibergall, M. B.; Lipscomb, J. D.; Solomon, E. I. *J. Am. Chem. Soc.* **2007**, *129*, 7427–7438.
(8) (a) Lundberg, M.; Morokuma, K. *J. Phys. Chem. B* **2007**, *111*, 9380–9389. (b) Lundberg, M.; Siegbahn, P. E. M.; Morokuma, K. *Biochemistry* **2008**, *47*, 1031–1042. (c) Lundberg, M.; Kawatsu, T.; Vreven, T.; Frisch, M. J.; Morokuma, K. *J. Chem. Theor. Comput.* **2009**, *5*, 222–234.
(9) Yan, F.; Munos, J. W.; Liu, P.; Liu, H. W. *Biochemistry* **2006**, *45*, 11473–11481.
(10) Mirica, L. M.; McCusker, K. P.; Munos, J. W.; Liu, H.-w.; Klinman, J. P. *J. Am. Chem. Soc.* **2008**, *130*, 8122–8123.
(11) (a) Price, J. C.; Barr, E. W.; Tirupati, B.; Bollinger, J. M., Jr.; Krebs, C. *Biochemistry* **2003**, *42*, 7497–7508. (b) Price, J. C.; Barr, E. W.; Glass, T. E.; Krebs, C.; Bollinger, J. M., Jr. *J. Am. Chem. Soc.* **2003**, *125*, 13008–13009. (c) Riggs-Gelasco, P. J.; Price, J. C.; Guyer, R. B.; Brehm, J. H.; Barr, E. W.; Bollinger, J. M., Jr.; Krebs, C. *J. Am. Chem. Soc.* **2004**, *126*, 8108–8109.
(12) Denisov, I. G.; Makris, T. M.; Sligar, S. G.; Schlichting, I. *Chem. Rev.* **2005**, *105*, 2253–2277.
(13) (a) Meunier, B.; de Visser, S. P.; Shaik, S. *Chem. Rev.* **2004**, *104*, 3947–3980. (b) Shaik, S.; Kumar, D.; de Visser, S. P.; Altun, A.; Thiel, W. *Chem. Rev.* **2005**, *105*, 2279–2328. (c) Shaik, S.; Cohen, S.; Wang, Y.; Chen, H.; Kumar, D.; Thiel, W. *Chem. Rev.* **2010**, *110*, 949–1017.

Scheme 1. HEPD-Catalyzed Reaction

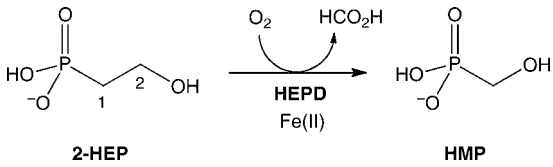

2-HEP **HMP**

strates using high-valent oxoiron(IV) (ferryl) intermediates.[14,15] In TauD, ferric superoxide reacts with α-ketoglutarate prior to ferryl formation.

Recently, Cicchillo et al. performed a series of structural and mechanistic studies of hydroxyethylphosphonate dioxygenase (HEPD).[16] HEPD utilizes Fe^{2+} and O_2 to cleave the C−C bond of 2-HEP, yielding hydroxymethylphosphonate (HMP) and formic acid (Scheme 1). 2-HEP and HMP were shown to be intermediates in the biosynthesis of phosphinothricin, which is a key structural component of some commercial herbicides.[17] In the X-ray crystal structures of HEPD, 2-hydroxyethylphosphonate (2-HEP) coordinated to the metal center in a bidentate manner using one of the phosphonate oxygen atoms and the hydroxyl oxygen. It was suggested that the first step of the HEPD-catalyzed substrate reaction should be H-abstraction from C2 of the substrate by a ferric superoxide intermediate. The specific C−C bond cleaved is that between C1 and C2, and this results in conversion of the C2 part of 2-HEP to formic acid, as revealed by their isotope labeling studies.

HEPD is similar to MIOX in that both enzymes cleave a C−C bond of the substrate. Moreover, it is likely that the first step of the HEPD reaction is, as with MIOX, H-abstraction by a ferric superoxide intermediate. Therefore, the catalytic mechanism of HEPD would presumably be similar to that of MIOX. However, the mechanism of HEPD, especially after the H-abstraction step, is still largely uncertain. We have recently investigated the catalytic mechanism of MIOX by means of computational chemistry and proposed that the O−O bond cleavage is the rate-limiting step.[6]

In an effort to elucidate the mechanism of the HEPD reaction and identify similarities and dissimilarities between HEPD and MIOX, we performed a series of density functional theory (DFT) calculations on an active-site model of the enzyme. The calculations indicated that, while the reaction of HEPD is somewhat similar to that of MIOX, the reactions differ from each other in several ways. Interestingly, our results suggest that HEPD uses a ferric hydroxide intermediate in the last step of the reaction. The HEPD mechanism thus has some resemblance to the lipoxygenase mechanism that uses a ferric hydroxide intermediate for H-abstraction, although the reaction mode of the ferric hydroxide intermediate in HEPD is more similar to the radical rebound process in P450 reactions.

2. Computational Methods

The Gaussian 09 program was used to perform all DFT calculations.[18] The quintet and septet spin states were taken into consideration. The B3LYP DFT functional[19] was used in conjunction with two basis sets, B1 and B2. B1 is a combination of the SDD effective core potential basis set[20] used for Fe and the 6-31G* basis set[21] for the rest of the atoms, and this was used for geometry optimizations. Final energies were obtained from single-point calculations with B2, which employs the TZVP basis set[22] for all atoms. Molecular geometries were drawn using the VMD software.[23] Throughout this paper, B3LYP/B2//B1 energies are reported, while B3LYP/B1 results are presented for the geometries and Mulliken spin distributions.

The X-ray structure determined by Cicchillo et al. at 1.92 Å resolution (PDB code 3GBF, see Figure 1a) was used as the starting point for our theoretical modeling.[16a] An active-site model (Figure 1b) was constructed and used in this study. The 2-HEP substrate and amino acid residues in the first coordination sphere were taken from the X-ray structure, and the Cd^{2+} ion present at the metal binding side was replaced with iron. An oxygen molecule was placed above the iron center. Hydrogen atoms were added as appropriate to the system, as described in Figure 1b. Because there was a short distance (2.64 Å) between the hydroxyl oxygen of 2-HEP and one of the carboxylate oxygen atoms of Glu176, it is likely that there is a proton between the two oxygen atoms. Therefore, we assumed that the hydroxyl oxygen of 2-HEP was not ionized but neutral. To avoid potential drastic movement of the ligands, the three atoms labeled with asterisks (C_β of His129, Glu176, and His182) were fixed at the positions in the X-ray structure. Frequency calculations were performed to characterize the energy-minimum and transition-state (TS) geometries, with these three atoms frozen. Energy-minimum geometries had only real frequencies, while TS geometries had an imaginary frequency corresponding to the relevant reaction coordinate. With this method, zero-point energy (ZPE) is not rigorously evaluated. Therefore, vibrational ZPE corrections were not made for the energy data presented here. Nevertheless, to obtain a rough estimate of the ZPE effect, ZPE-corrected values were reported in the Supporting Information (Table S1). The effect of Tyr98 was also taken into account for some of the reaction steps, to verify that it does not affect the relative stability of the hydroperoxylation and hydroxylation pathways. When Tyr98 was included in the calculation model, the C_β atom of this residue was fixed at the position in the X-ray structure.

3. Results and Discussion

3.1. Overview of the Mechanism. We propose, on the basis of our calculations, that the reaction occurs in four major steps. The overall reaction energy profile is presented in Figure 2. The reaction starts with H-abstraction from C2 of 2-HEP by the superoxide moiety of the reactant complex (**RC**) to form an Fe(II)-OOH intermediate (**Int-ooh**). This step was found to have the highest energy barrier in the reaction, and we predict that this step is rate-limiting. In the second step, **Int-ooh** can follow two possible pathways that involve hydroperoxylation and

(14) Krebs, C.; Fujimori, D. G.; Walsh, C. T.; Bollinger, J. M., Jr. *Acc. Chem. Res.* **2007**, *40*, 484–492.
(15) (a) Shaik, S.; Hirao, H.; Kumar, D. *Acc. Chem. Res.* **2007**, *40*, 532–542. (b) Shaik, S.; Hirao, H.; Kumar, D. *Nat. Prod. Rep.* **2007**, *24*, 533–552.
(16) (a) Cicchillo, R. M.; Zhang, H.; Blodgett, J. A. V.; Whitteck, J. T.; Li, G.; Nair, S. K.; van der Donk, W. A.; Metcalf, W. W. *Nature* **2009**, *459*, 871–875. (b) Whitteck, J. T.; Cicchillo, R. M.; van der Donk, W. A. *J. Am. Chem. Soc.* **2009**, *131*, 16225–16232.
(17) Blodgett, J. A. V.; Thomas, P. M.; Li, G.; Velasquez, J. E.; van der Donk, W. A.; Kelleher, N. L.; Metcalf, W. W. *Nature Chem. Biol.* **2007**, *3*, 480–485.
(18) Frisch, M. J.; et al. *Gaussian 09*, revision A.02; Gaussian, Inc.: Wallingford CT, 2009.
(19) (a) Becke, A. D. *J. Chem. Phys.* **1993**, *98*, 5648–5652. (b) Lee, C.; Yang, W.; Parr, R. G. *Phys. Rev. B* **1988**, *37*, 785–789. (c) Vosko, S. H.; Wilk, L.; Nusair, M. *Can. J. Phys.* **1980**, *58*, 1200–1211.
(20) Dolg, M.; Wedig, U.; Stoll, H.; Preuss, H. *J. Chem. Phys.* **1987**, *86*, 866–872.
(21) Hehre, W.; Radom, L.; Schleyer, P. v. R.; Pople, J. A. *Ab Initio Molecular Orbital Theory*; John Wiley & Sons: New York, 1986.
(22) Schäfer, A.; Huber, C.; Ahlrichs, R. *J. Chem. Phys.* **1994**, *100*, 5829–5835.
(23) Humphrey, W.; Dalke, A.; Schulten, K. *J. Mol. Graphics* **1996**, *14*, 33–38.

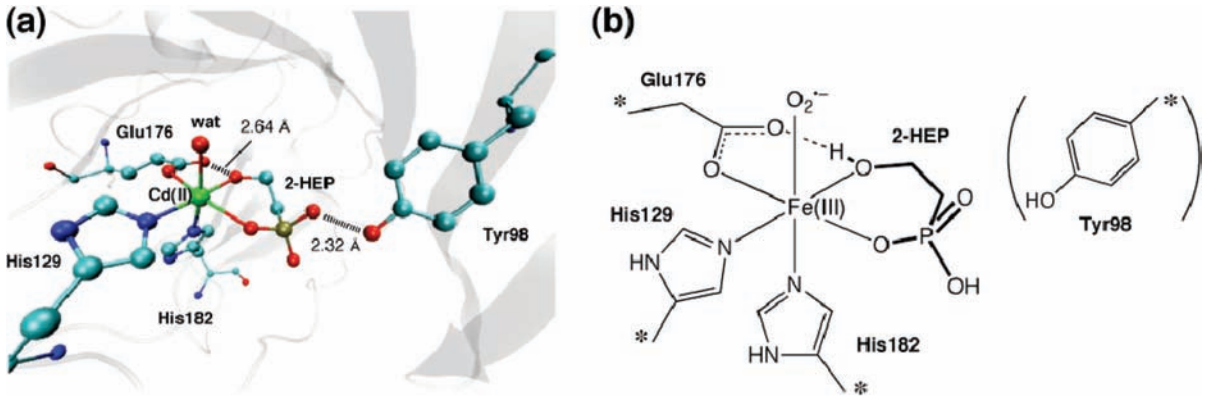

Figure 1. (a) Active-site structures of HEPD (PDB code 3GBF). (b) Active-site model employed in this study. The hydrogen atoms on carbon atoms are not shown explicitly. The atoms marked with asterisks were frozen in geometry optimizations. Tyr98 was included only in special cases.

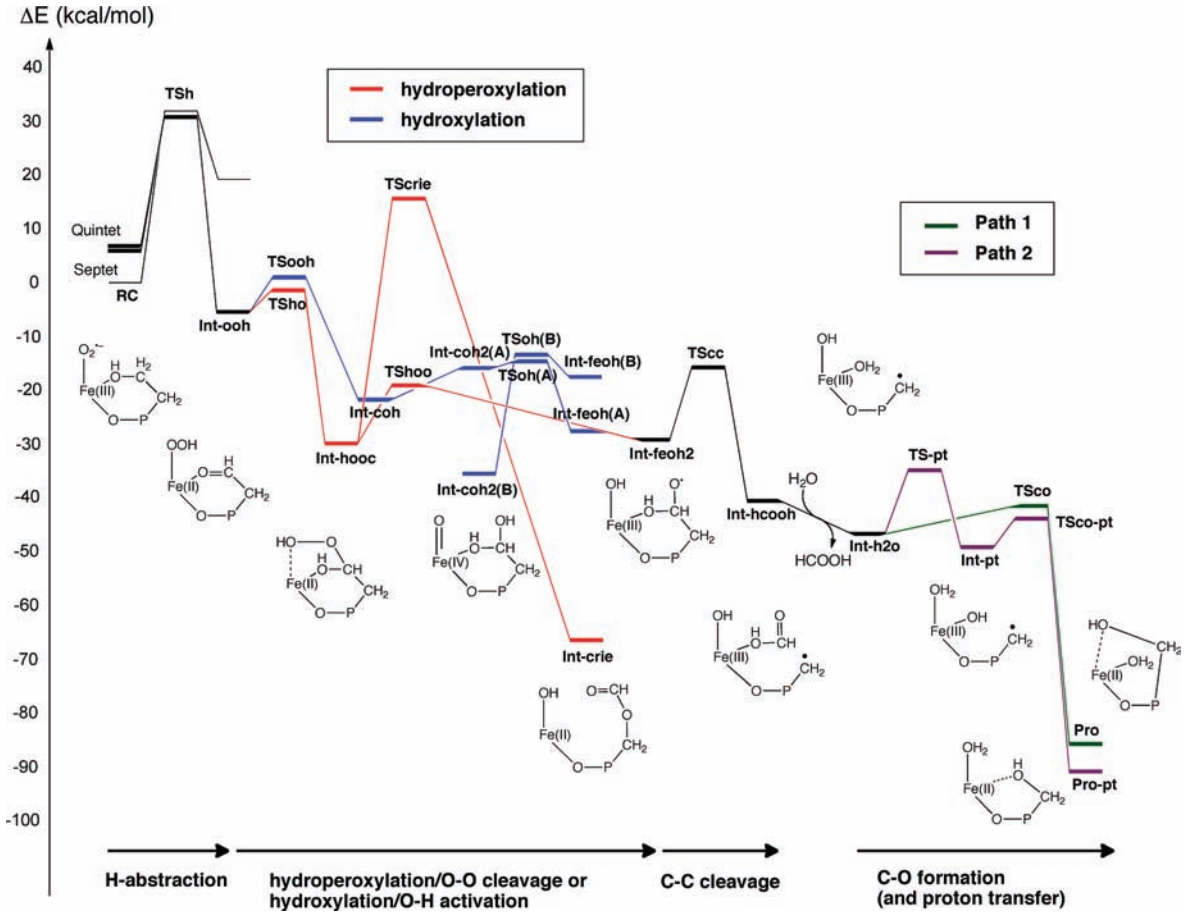

Figure 2. The entire reaction energy profile (in kcal/mol) obtained at the B3LYP/B2//B1 level of theory.

Scheme 2. Gem-Diol Radical That Is Likely Formed during the HEPD-Catalyzed Reaction

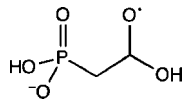

hydroxylation, respectively. Both pathways lead to a complexation of a ferric hydroxide with a gem-diol radical (**Int-feoh2**, see Scheme 2). A Criegee-type rearrangement in the hydroperoxylation pathway via **TScrie** has a very high barrier and is not energetically feasible. The C1−C2 bond of this complex is then cleaved to generate a ferric hydroxide species to which formic acid and a $^{\bullet}CH_2PO_2(OH)^-$ substrate radical are bound (**Int-hcooh**). We assume that the formic acid molecule present in **Int-hcooh** will be replaced with a water molecule to yield **Int-h2o**. The C1 methylene part of the substrate in **Int-h2o** has a radical character, and this is likely to attack the ferric hydroxide moiety. Finally, the product complex **Pro** or **Pro-pt** is formed, depending on whether the reaction followed path 1 or path 2, respectively. In the product complexes, HMP is bound to the ferrous center. The individual steps are discussed in more detail in the following sections.

3.2. Ferric Superoxide and Its H-Abstraction in the First Step. The geometry of **RC** containing a ferric superoxide moiety was optimized at the B3LYP/B1 level for the quintet and septet spin states. As shown in Figure 3, side-on and end-on geometries

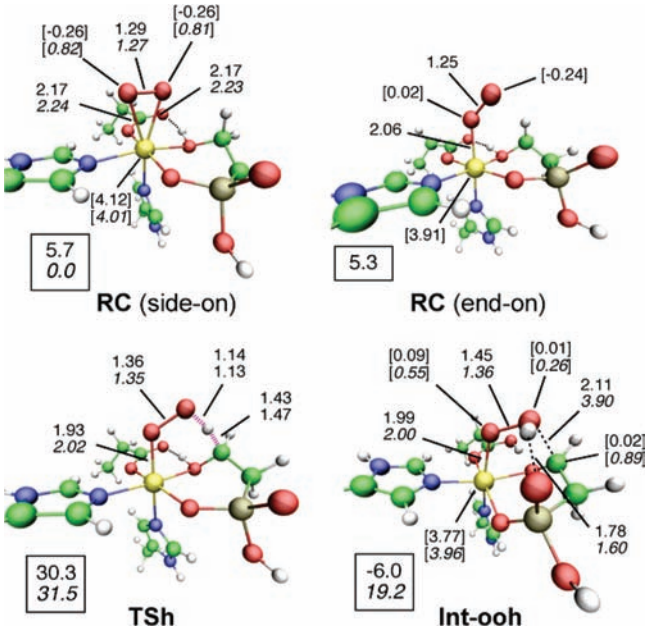

Figure 3. Optimized geometries of key species appearing during the H-abstraction step obtained for the quintet (plain font) and septet (italic font) states. Bond distances are in Å. The values in boxes are the relative energies (in kcal/mol) with respect to the septet ground state of the reactant complex **RC**. The key atomic spin population values are presented in square brackets.

were obtained for **RC** as local energy minima.[24] In both the quintet and septet states, the iron center formally possessed five unpaired electrons in the d-type molecular orbitals (MOs) of iron, which were antiferromagnetically (quintet) or ferromagnetically (septet) coupled to the unpaired electron in the superoxide moiety. The spin population value (ρ) of the coordinating O_2 moiety was −0.52 (quintet, side-on), −0.22 (quintet, end-on), or 1.63 (septet), which indicates that <1 electron shifted from Fe(II) to the molecular oxygen upon O_2 coordination. Reflecting the different spin-coupling modes, the Fe−O bond of the side-on geometry in the quintet state was shorter than that in the septet state by 0.06−0.07 Å. The septet state of **RC** was calculated to be lower in energy than the quintet state by >5 kcal/mol, which suggests that the septet state is the ground state at the beginning of the HEPD reaction.

To abstract a hydrogen atom, one of the oxygen atoms in the superoxide moiety approaches the nearby hydrogen atom on C2 of 2-HEP. Transition states (**TSh**) were located for the H-abstraction step in both the quintet and septet states. For **TSh**, the quintet state was slightly lower in energy than the septet state. Thus, despite the low energy of the septet state at the beginning, the spin-state ordering was inverted just before **TSh**. After **TSh**, the intermediate **Int-ooh** forms. The calculated barrier for H-abstraction was 30.3 kcal/mol. This seems to be a bit too high, but the ZPE effect lowers the barrier by >4 kcal/mol (Table S1). We assumed in this study that the hydroxyl group of 2-HEP is not deprotonated, because it is deemed natural to assume that there is a proton between the hydroxyl oxygen and the nearby carboxylate oxygen of Glu176. Nevertheless, we also examined the case where there is no proton between the hydroxyl oxygen of 2-HEP and the glutamate oxygen of Glu176. Geometry optimization of **RC** with a deprotonated

(24) Optimization of an end-on geometry in the septet state resulted in dissociation of O_2 from iron.

Scheme 3. Two Possible Reaction Pathways from **Int-ooh**[a]

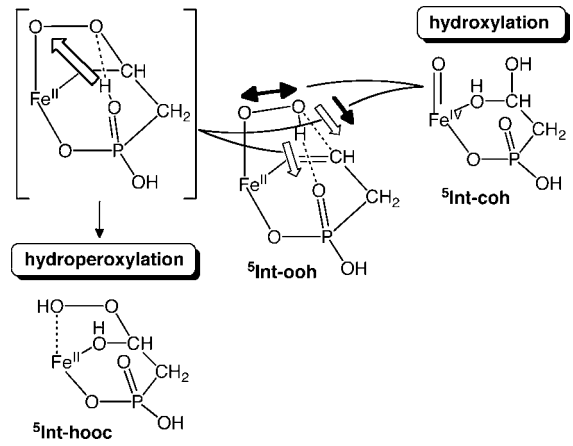

[a] The arrows schematically indicate how atoms move in subsequent steps.

hydroxyl group resulted in a large movement of the carboxylate moiety of Glu176, but the H-abstraction barrier was lowered to 18.1 kcal/mol (Table S1).

Because an electron gained from the abstracted hydrogen atom forms a bond pair with the unpaired electron in the superoxide moiety, one may assume that the resultant species is Fe(III)-OOH, with an unpaired electron left behind and localized on the C2 site. However, in the quintet state the unpaired electron on C2 was transferred into the Fe center through the coordinating hydroxyl oxygen. No unpaired electron remained on the substrate moiety, as can be seen from the ρ value of 0.02 for C2 (Figure 3). As a consequence, one of the Fe d-MOs is doubly occupied. The iron center is thus reduced to Fe(II), and the C2 part of the substrate is described here as a formyl group. Because the hydroxyl group now has strong double bond character (C═O), the hydroxyl proton originally on the substrate is donated to the carboxylate oxygen of Glu176 at **Int-ooh**. In the septet state, however, such electron transfer to Fe did not occur, and the ρ value on C2 was 0.89 (Figure 3). Unlike the quintet case, the hydroxyl proton remained on the substrate at ^{7}**Int-ooh**. Because of the spin localization on C2 in the septet state, the distal oxygen atom in the Fe-OOH moiety and C2 in **Int-ooh** repel each other. In fact, the distance between these moieties is much longer (3.90 Å) than that for the quintet state (2.11 Å) (Figure 3). Essentially the same electron reorganization processes were observed in earlier studies of IPNS[8b] and MIOX.[6] **Int-ooh** was much more stable in the quintet state than in the septet state. Thus, the reactions should lead exclusively to ^{5}**Int-ooh**. Interestingly, at this stage, the abstracted hydrogen atom in the Fe-OOH moiety favorably interacted with one of the phosphonate oxygen atoms through H-bonding (Figure 3).

3.3. Hydroperoxylation and Hydroxylation in the Second Step. After formation of **Int-ooh**, the reaction pathway was found to bifurcate (Scheme 3). The two reaction pathways, hydroperoxylation and hydroxylation, are discussed in detail below. As shown in Figure 2, the hydroperoxylation pathway is energetically more favorable than the hydroxylation pathway. The difference in the barrier height between the two pathways is 2.1 kcal/mol. ZPE correction further increases the energy gap to 4.2 kcal/mol (Table S1).

3.3.1. Hydroperoxylation Pathway. The hydroperoxylation pathway is associated with the formation of a hydroperoxylated intermediate, which is initiated by proton transfer (PT) to the closest phosphonate oxygen. This PT was accompanied by C−O

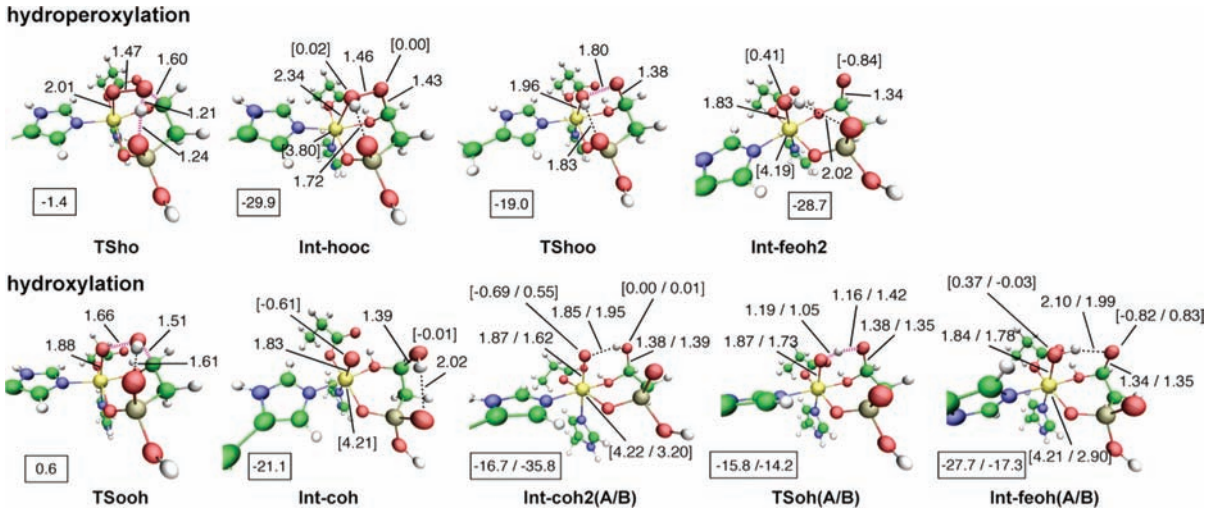

Figure 4. Optimized geometries of key species appearing during the second step in the quintet state. Bond distances are in Å. The values in boxes are the relative energies (in kcal/mol), with respect to the septet ground state of the reactant complex **RC**. The two values presented for **Int-coh2**, **TSoh**, and **Int-feoh** are for two states (**A**/**B**) with different orbital occupancies. The key atomic spin population values are presented in square brackets.

bond formation between the distal oxygen and C2 and donation of the hydroxyl proton, which temporarily stayed on Glu176, back to the substrate. An analogous PT-assisted C−O bond formation was observed in our previous study of MIOX.[6] In the MIOX reaction, the transferred proton remained on the hydroxide base. However, a slightly different mechanism was observed here, with immediate shuttling of the transferred proton back to the proximal oxygen to produce a ferrous-alkylhydroperoxo intermediate, **Int-hooc** (see also Figure S9 in the Supporting Information). The difference in the proton retention behavior between HEPD and MIOX can be attributed to the different basicities of the relevant bases. The basicity of the bridging hydroxide of MIOX is enhanced by an aspartate residue in its immediate vicinity. Compared to the hydroxide in MIOX, the basicity of the phosphonate oxygen in HEPD is low. This low basicity does not allow retention of the proton on the base. Another major difference between HEPD and MIOX is the oxidation state of the iron center of **Int-ooh**. As discussed earlier, additional electron reorganization gives an Fe oxidation state of +2 for **Int-ooh** in HEPD, whereas in the corresponding MIOX species the Fe oxidation state is +3. This difference occurs because HEPD is a mononuclear enzyme, while MIOX is a dinuclear enzyme. Thus, although electron reorganization and reduction of iron do occur in MIOX, these take place on the other iron rather than the one to which the OOH moiety is bound.[6] The iron oxidation state of +2 makes the Fe-OOH moiety of HEPD more electron rich and basic; thus it accepts a proton more easily. All these factors facilitate the formation of **Int-hooc** in HEPD.

The hydroperoxylation mechanism usually assumes migration of the proximal oxygen of the OOH group from the iron center to the substrate. However, the present hydroperoxylation mechanism does not require migration of the proximal oxygen. Instead, the oxygen atoms in the hydroperoxo unit retain the original arrangement, and only the proton shuttling from the distal oxygen to the proximal oxygen via the phosphonate oxygen is required. Even in the resultant **Int-hooc**, the Fe−O distance was 2.34 Å; thus, the proximal oxygen does not completely dissociate from the iron center (Figure 4). Interestingly, the O−O bond of **Int-hooc** was found to undergo homolytic cleavage via the transition state **TShoo** with an energy barrier of only 10.9 kcal/mol. The resultant **Int-feoh2** contained a ferric hydroxide moiety as well as a gem-diol radical.

Scheme 4. Schematic Illustration of the Electron Reorganization Process for the Step from **Int-coh2(A)** to **Int-feoh(A)**[a]

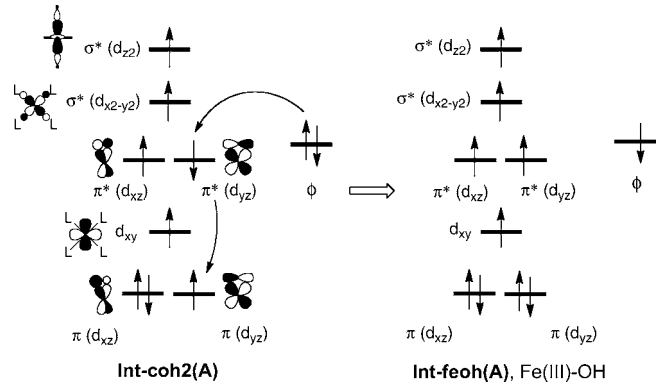

[a] ϕ indicates the relevant orbital of the substrate.

3.3.2. Hydroxylation Pathway. The other pathway involves concerted C−O bond formation and O−O bond cleavage. This pathway can be regarded as a hydroxylation pathway because it generates an intermediate **Int-coh** containing a hydroxylated substrate via the transition state, **TSooh** (see Figure 4). **Int-coh** is converted to **Int-coh2(A)** via a slight change in the H-bond pattern of the hydroxyl group. **Int-coh2(A)** had a little unusual orbital occupancy pattern, which can be formally described as five spin-up electrons in iron d-MOs and a spin-down electron in the π^* MO (Scheme 4 and Figure S10 in the Supporting Information). A hydrogen atom of one of the hydroxyl groups of the gem-diol in **Int-coh2(A)** is abstracted by the FeO moiety. This H-abstraction step passes through a transition state (**TSoh(A)**), and a ferric hydroxide/gem-diol radical intermediate (**Int-feoh(A)**) is formed. The barrier for this step was only 0.9 kcal/mol. The iron center of **Int-feoh(A)** has five unpaired spin-up electrons in the d-MOs and a ρ value of 4.21, which is typical for Fe(III).[25] **Int-feoh(A)** is subsequently converted to more stable **Int-feoh2** by rearrangement of the H-bonding pattern.

(25) Blomberg, M. R. A.; Siegbahn, P. E. M. *Theor. Chem. Acc.* **1997**, *97*, 72–80.

Scheme 5. Two Possible Electron Rearrangements for the Step from **Int-coh2(B)** to **Int-feoh(B)**: (a) Exchange-Enhanced and (b) Exchange-Damped Reactions for the Reactions of Ferryl Species[a]

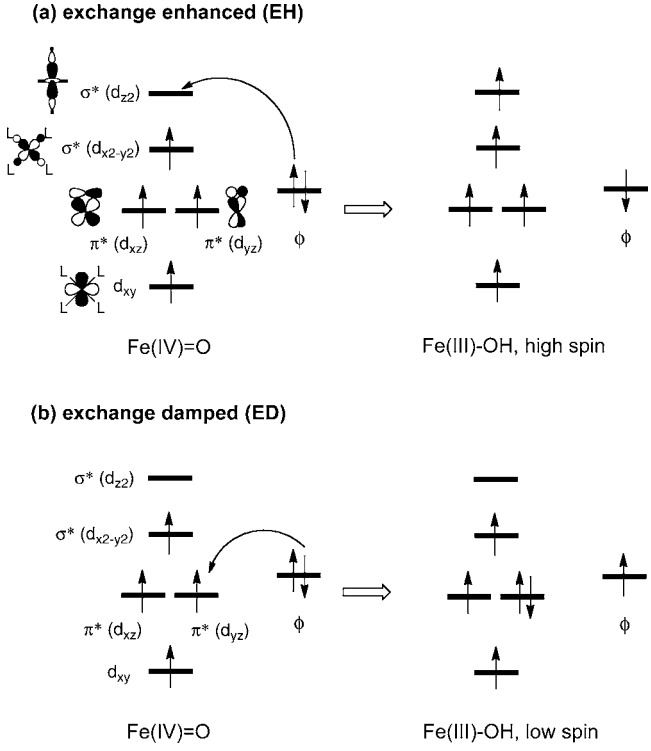

[a] ϕ indicates the relevant orbital of the substrate.

Another state, **Int-coh2(B)**, had a different orbital occupancy pattern in which four unpaired spin-up electrons populated the d-MOs. **Int-coh2(B)** was not smoothly connected to the preceding intermediates on the potential energy surface, but it was 19.1 kcal/mol more stable than **Int-coh2(A)** (Figure 2). **Int-coh2(B)** is characterized as a complex containing ferryl (Fe(IV)═O) and a neutral gem-diol. In bioinorganic chemistry, ferryl is known to have powerful H-abstraction ability. In fact, we were able to determine a reaction path in which the ferryl moiety in **Int-coh2(B)** abstracted a hydrogen atom from the O−H bond of the substrate. However, the barrier for the H-abstraction was as high as 21.6 kcal/mol, and **TSoh(B)** was higher in energy than **TSoh(A)** by 1.6 kcal/mol. The inefficient H-abstraction in **Int-coh2(B)** can be understood by the concepts of "exchange-enhanced (EH)" and "exchange-damped (ED)" reactions (Scheme 5). It has been theoretically verified in many systems that high-spin ferryl-containing complexes tend to undergo EH reactions.[26−28] The EH reaction is associated with an electron shift from the substrate orbital (ϕ) to the vacant d_{z^2}-type σ^* orbital of the iron center (Scheme 5a). The resultant species therefore has five spin-up electrons in the d-MOs. This process increases the number of unpaired electrons on iron, and thus the system gains exchange stabilization.[29] By contrast, the ED reaction (Scheme 5b) involves an electron shift from the substrate to one of the singly occupied π^* MOs. This decreases the number of unpaired parallel-spin electrons on the iron center. Unlike many other reactions of high-spin ferryl species, the H-abstraction by the ferryl intermediate (from **Int-coh2(B)** to **Int-feoh(B)**) was found to undergo an ED reaction in the present case. This is attributed to steric restraint imposed on the ligand. The EH reaction typically necessitates a collinear arrangement of the O−H (or C−H) bond and the Fe(IV)═O bond to achieve an efficient overlap between the metal d_{z^2}-type σ^* orbital and the substrate ϕ orbital. In other words, the activated bond has to stand upright just above the Fe(IV)═O bond. However, the steric restraint in HEPD allows only a small Fe−O−H angle and not the EH required arrangement. The bent Fe−O−H arrangement is favorable for the ED reaction, which requires an overlap between the metal-oxo π^* orbital and the substrate ϕ orbital. As such, the ferryl intermediate **Int-coh2(B)** is forced to undergo the ED reaction with a high activation energy barrier. The ED reaction leads to a low-spin iron center after H-abstraction at **Int-feoh(B)** (ρ = 2.90). This low-spin state is much less stable than the high-spin counterpart (**Int-feoh(A)**), as can be seen in Figure 2.

3.3.3. Effect of Tyr98. Inspection of the crystal structure reveals that the phosphonate oxygen, which plays a critical role in the hydroperoxylation pathway, forms a H-bond with the hydroxyl group of Tyr98 (Figure 1a). This H-bond effect may restrict the movement of the phosphonate oxygen and may thereby result in a diminished effect of the phosphonate oxygen as a pivot for the proton shuttling. If this is the case, the preference between the hydroperoxylation and hydroxylation pathways may be altered. To examine its possibility, we compared the step from ^{5}**Int-ooh** to ^{5}**Int-hooc** (hydroperoxylation) and the step from ^{5}**Int-ooh** to ^{5}**Int-coh** (hydroxylation). The results show that the barrier for the former is still lower by 1.6 kcal/mol, even if the effect of Tyr98 is taken into consideration (Table S1). It thus seems unlikely that Tyr98 alters the mechanistic preference, although more accurate studies based on QM/MM methods are needed to derive definitive conclusions.

3.4. C−C Cleavage in the Third Step. Both hydroperoxylation and hydroxylation result in **Int-feoh2** formation from **Int-ooh** (Figure 2). The gem-diol radical species in **Int-feoh2** easily undergoes homolytic C−C bond cleavage through transition state **TScc** to yield an intermediate containing R-CH$^\bullet$ and HCOOH (**Int-hcooh**, Figure 5). At this point, one of the products of the HEPD reaction, namely formic acid, is formed.

3.5. Comparison of the Present Study to an Earlier Study. While the hydroperoxylation and hydroxylation mechanisms were previously proposed by Cicchillo et al.,[16] our proposed mechanisms appear to differ somewhat from theirs. Their proposed mechanism assumed a Criegee-type rearrangement of the substrate in the ferrous-alkylhydroperoxo intermediate (**Int-hooc**) for the hydroperoxylation pathway or heterolytic C−C bond cleavage in the ferryl-gem-diol intermediate (**Int-coh2(B)**) for the hydroxylation pathway. The Criegee-type rearrangement is associated with formation of a C−O bond between C1 and the distal oxygen, heterolytic C−C bond cleavage, and heterolytic O−O bond cleavage.[16] The optimized geometries of the transition state for this process, **TScrie**, and the subsequently

(26) An exchange-enhanced reaction was first found by one of the present authors (H.H.) with Prof. Sason Shaik for the reactions of cytochrome P450 compound I, and essentially the same trends were observed in the reactions of other ferryl intermediates: Hirao, H.; Kumar, D.; Thiel, W.; Shaik, S. *J. Am. Chem. Soc.* **2005**, *127*, 13007–13018.

(27) (a) Kumar, D.; Hirao, H.; Que, L., Jr.; Shaik, S. *J. Am. Chem. Soc.* **2005**, *127*, 8026–8027. (b) Hirao, H.; Kumar, D.; Que, L., Jr.; Shaik, S. *J. Am. Chem. Soc.* **2006**, *128*, 8590–8606. (c) Hirao, H.; Que, L., Jr.; Nam, W.; Shaik, S. *Chem. Eur. J.* **2008**, *14*, 1740–1756. (d) Hirao, H.; Chen, H.; Carvajal, M. A.; Wang, Y.; Shaik, S. *J. Am. Chem. Soc.* **2008**, *130*, 3319–3327.

(28) For recent discussion about exchange-enhanced reactions, see for example: (a) Chen, H.; Lai, W. Z.; Shaik, S. *J. Phys. Chem. Lett.* **2010**, *1*, 1533–1540. (b) Geng, C. Y.; Ye, S.; Neese, F. *Angew. Chem., Int. Ed.* **2010**, *49*, 5717–5720.

(29) Carter, E. A.; Goddard, W. A. *J. Phys. Chem.* **1988**, *92*, 5679–5683.

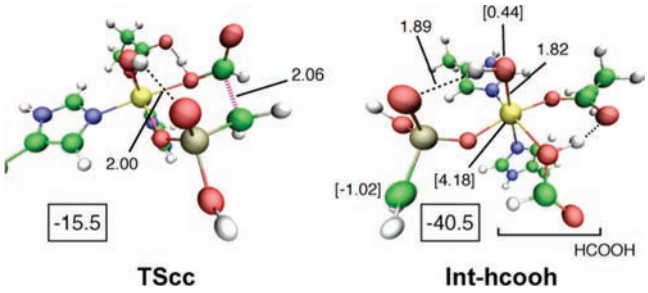

Figure 5. Optimized geometries of key species appearing during the third step in the quintet state. Bond distances are in Å. The values in boxes are the relative energies (in kcal/mol) with respect to the septet ground state of the reactant complex **RC**. The key atomic spin population values are presented in square brackets.

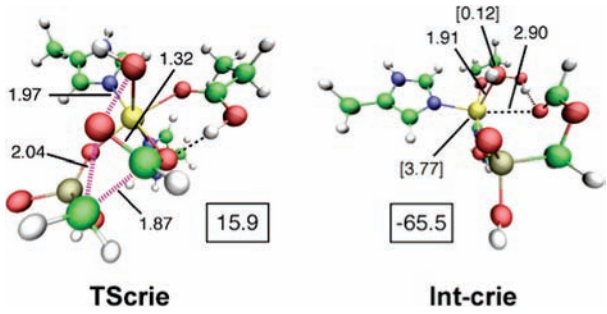

Figure 6. Optimized geometries for a Criegee-type rearrangement in the quintet state. Bond distances are in Å. The values in boxes are the relative energies (in kcal/mol), with respect to the septet ground state of the reactant complex **RC**. The key atomic spin population values are presented in square brackets.

formed intermediate, **Int-crie**, are shown in Figure 6. Our calculations show that this process involves a high barrier (45.9 kcal/mol) and is thus energetically unfavorable (Figure 2). As the ρ value (3.77) of Fe implies, the oxidation state of Fe is +2 at **Int-crie**, which is consistent with the hypothesis that the O−O bond cleavage should be heterolytic. Heterolytic C−C bond cleavage of **Int-coh2(B)** in the hydroxylation pathway also requires a large energy increase (Figure S12, Supporting Information). Our calculations therefore do not support these heterolytic mechanisms.

Instead, our calculations favor the mechanism in which a gem-diol radical (**Int-feoh2**) is initially formed via a homolytic O−O bond cleavage of **Int-hooc**, the energy barrier for which is only 10.9 kcal/mol, and then homolytic C−C cleavage takes place. In the case of the HEPD reaction, the homolytic C−C bond cleavage gives rise to a R-$CH_2^{\bullet}$ radical and formic acid with a carbonyl bond. The C−C bond cleavage of the gem-diol radical allows for spin pairing or bond formation between the unpaired electron on the oxygen and the unpaired electron on C2 (eq 1).

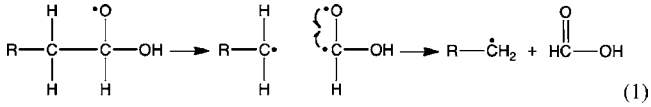

Similar C−C bond cleavage preceded by the formation of a gem-diol radical was observed in our previous study of the MIOX reaction.[6] The energy barrier for the process from **Int-feoh2** to **Int-hcooh** was only 13.3 kcal/mol. **Int-feoh2** contains a ferric hydroxide unit complexed with a gem-diol radical. Formation of an analogous ferric/gem-diol radical intermediate was previously suggested by Siegbahn and co-workers for the reaction of extradiol dioxygenases such as homoprotocatechuate 2,3-dioxygenase (HPCD) on the basis of their DFT results.[30] Furthermore, an X-ray crystal structure for a gem-diol radical was solved for HPCD by Kovaleva and Lipscomb.[31]

3.6. C−O Bond Formation (and Proton Transfer) in the Fourth Step. It can be assumed that the formic acid produced in the previous step may be displaced by a water molecule that occupies the position where the formic acid was. In support of this hypothesis, this ligand exchange from **Int-hcooh** to **Int-h2o** was found to stabilize the system by 5.8 kcal/mol (Figure 2).

We examined two possible pathways extending from **Int-h2o** (Figure 7). Path 1 is associated with the attack of the $CH_2^{\bullet}$ moiety of the substrate radical on the axial OH of the ferric hydroxide. This step involves a transition state for C−O bond formation (**TSco**), and the energy barrier was calculated to be only 5.1 kcal/mol. In the resultant product complex **Pro**, the hydroxyl group of HMP occupied the axial site of the iron center. Path 2 involves proton transfer from the equatorial water ligand to the hydroxide ligand prior to the C−O bond formation. In this step, **Int-h2o** is converted to **Int-pt** via a proton-transfer transition state, **TSpt** (Figure 7). The energy barrier for this step was 11.9 kcal/mol. The hydroxide in **Int-pt** is in the equatorial site, and it seems to be easier for the $CH_2^{\bullet}$ moiety to access the hydroxide in path 2. The C−O bond formation in path 2 proceeds via the transition state **TSco-pt**. Although the resultant product complex (**Pro-pt**) was 5.4 kcal/mol lower in energy than **Pro**, the barrier for C−O bond formation in path 2 (5.2 kcal/mol) was as high as that for path 1. Thus, the two possible C−O bond formation processes from **Int-h2o** and **Int-pt** exhibit similar energetic trends. Considering the extra energy barrier of 11.9 kcal/mol that is required for proton transfer in path 2, it appears that path 1 is more favorable as the fourth step.

It is worth noting that a ferric hydroxide intermediate is also used in the catalytic reactions of lipoxygenases such as soybean lipoxygenase-1 (SLO-1), where ferric hydroxide is used as a reactive species to abstract hydrogen from a polyunsaturated fatty acid.[32] However, the reaction mode of the ferric hydroxide intermediate in HEPD is better characterized as radical coupling, similar to the rebound step of the hydroxylation reaction of cytochrome P450.[13]

3.7. Summary of the Newly Proposed Mechanism. On the basis of the results of our DFT calculations, we propose an enzymatic reaction mechanism for HEPD as illustrated in Scheme 6. In the first step of the reaction, the ferric superoxide **RC** abstracts one of the hydrogen atoms on C2 of 2-HEP. As a result, **Int-ooh** is produced, and then with the help of the phosphonate oxygen, simultaneous proton transfer from the distal to the proximal oxygen and C−O bond formation occur to give **Int-hooc**. The O−O bond of this intermediate is easily cleaved, and **Int-feoh2** is generated. The subsequent homolytic C−C bond cleavage leads to formation of formic acid and an

(30) (a) Siegbahn, P. E. M.; Haeffner, F. *J. Am. Chem. Soc.* **2004**, *126*, 8919–8932. (b) Borowski, T.; Georgiev, V.; Siegbahn, P. E. M. *J. Am. Chem. Soc.* **2005**, *127*, 17303–17314. (c) Borowski, T.; Georgiev, V.; Siegbahn, P. E. M. *J. Mol. Model.* **2010**, *11*, 1673–1677.
(31) Kovaleva, E. G.; Lipscomb, J. D. *Biochemistry* **2008**, *47*, 11168–1117.
(32) (a) Costas, M.; Mehn, M. P.; Jensen, M. P.; Que, L., Jr. *Chem. Rev.* **2004**, *104*, 939–986. (b) Solomon, E. I.; Brunold, T. C.; Davis, M. I.; Kemsley, J. N.; Lee, S.-K.; Lehnert, N.; Neese, F.; Skulan, A. J.; Yang, Y.-S.; Zhou, J. *Chem. Rev.* **2000**, *100*, 235–349. (c) Nelson, M. J.; Seitz, S. P. *Curr. Opin. Struct. Biol.* **1994**, *4*, 878–884. (d) Liang, Z. X.; Klinman, J. P. *Curr. Opin. Struct. Biol.* **2004**, *14*, 648–655. (e) Hammes-Schiffer, S. *Acc. Chem. Res.* **2006**, *39*, 93–100.

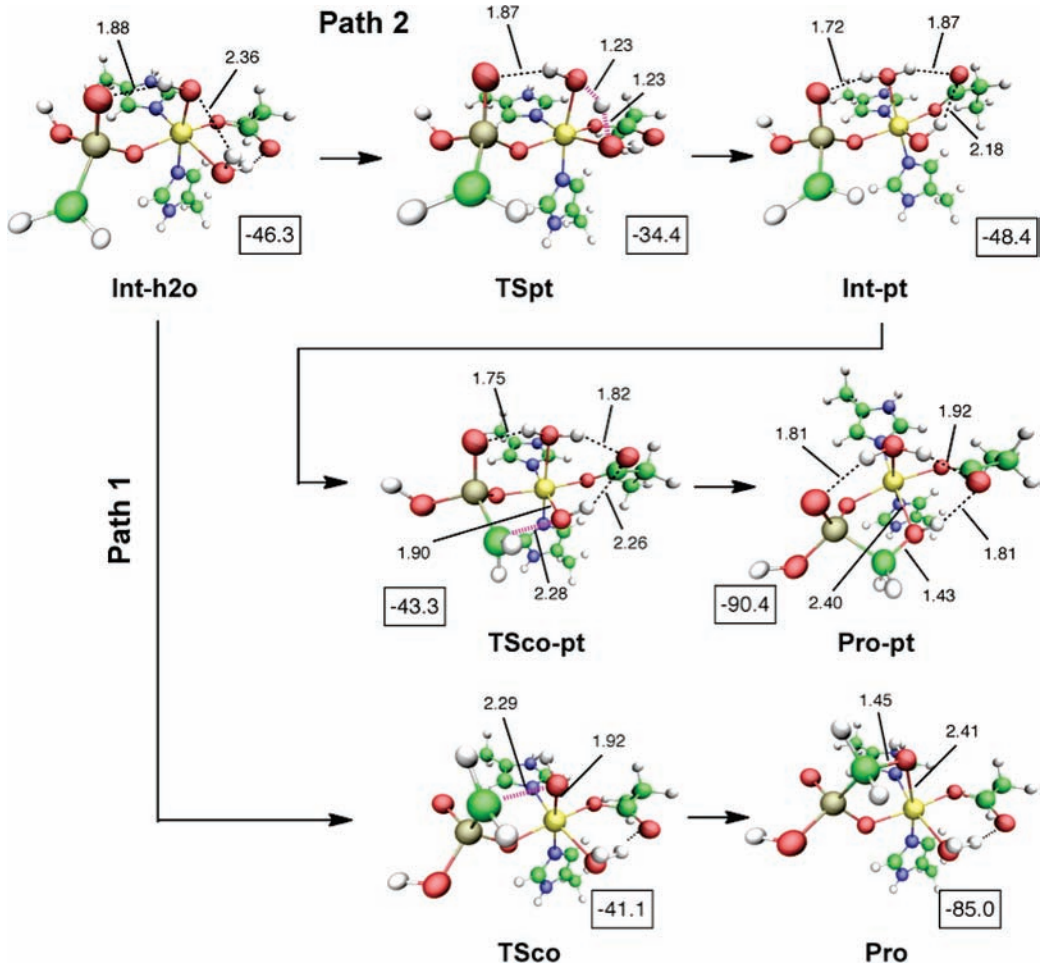

Figure 7. Optimized geometries of key species appearing during the fourth steps in the quintet state. Bond distances are in Å. The values in boxes are the relative energies in kcal/mol.

Scheme 6. Mechanism Proposed in the Present Work for the HEPD Reaction

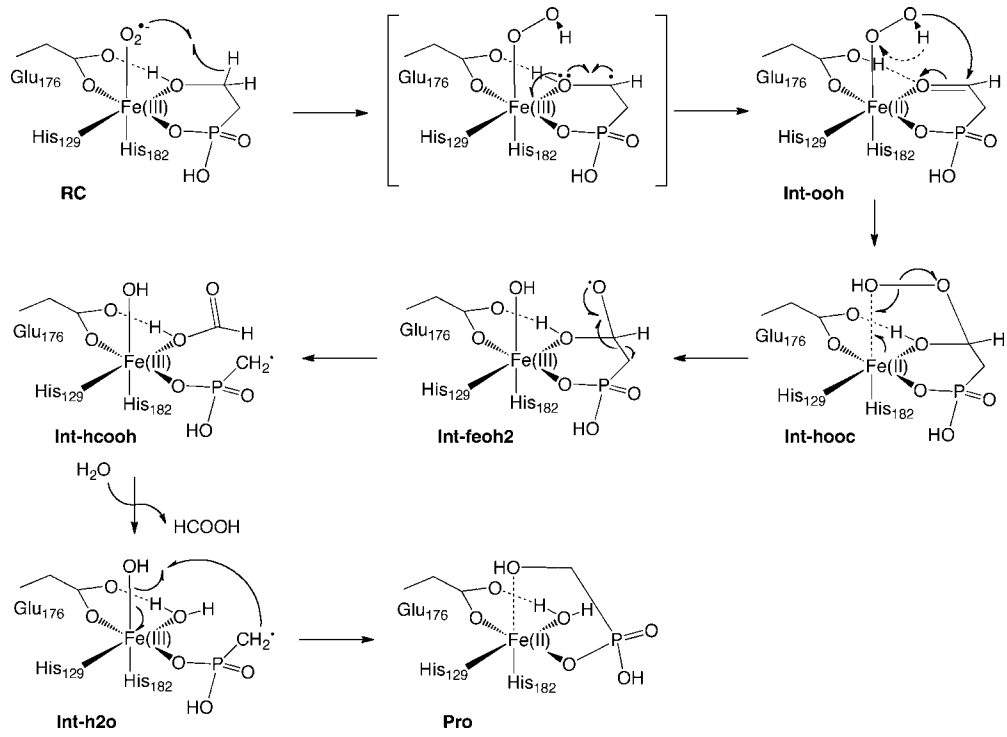

R-$CH_2^{\bullet}$ species. After replacement of HCOOH with H_2O, the substrate radical attacks the ferric hydroxide unit of the intermediate to produce HMP and complete the reaction.

4. Conclusion

DFT calculations on an enzyme active-site model were undertaken to examine the mechanism of the catalytic reaction of HEPD. The reaction pathways from 2-HEP to HMP were delineated on the basis of the calculation results. To initiate the reaction, a ferric superoxide intermediate abstracts a hydrogen atom from the C2 position of 2-HEP, in a manner similar to the H-abstraction in the MIOX-catalyzed reaction. The H-abstraction is the rate-limiting step. Afterward, the reaction proceeds via a hydroperoxylation pathway. The ferrous-alkylhydroperoxo intermediate in the hydroperoxylation pathway then undergoes homolytic O−O bond cleavage to give an intermediate containing ferric hydroxide and a gem-diol radical. Subsequent C−C bond cleavage leads to formation of a $^{\bullet}CH_2PO_2(OH)^-$ intermediate. The substrate radical then attacks the ferric hydroxide species to produce a HMP product. This study ignored the effect of the protein environment on the active-site events. Assessment of the environmental effect using the ONIOM(QM:MM) technique is an interesting research subject, albeit beyond the scope of this study. We are currently investigating environmental effects.

Acknowledgment. H.H. thanks the FIFC fellowship. This work was in part supported by a CREST grant in the Area of High Performance Computing for Multi-scale and Multi-physics Phenomena from the Japan Science and Technology Agency (JST). The computational resources at the Research Center for Computational Science at Institute for Molecular Science (RCCS-IMS) and Academic Center for Computing and Media Studies of Kyoto University are gratefully acknowledged.

Supporting Information Available: Complete ref 18, energy data, results of relaxed scan calculations, geometric changes after **TSho**, natural orbitals for **Int-coh2(A)**, energy changes with a Criegee-type rearrangement and heterolytic C−C cleavage, and Cartesian coordinates of all optimized geometries. This material is available free of charge via the Internet at http://pubs.acs.org.

JA108174D